Muscle carnitine availability plays a central role in regulating fuel metabolism in the rodent

Craig Porter[1], Dumitru Constantin-Teodosiu[†1*], Despina Constantin[1], Brendan Leighton[2], Simon M. Poucher[2] and Paul L. Greenhaff[1]

[1]MRC/ARUK Centre for Musculoskeletal Ageing Research, School of Life Sciences, University of Nottingham Medical School, Nottingham NG7 2UH, UK. [2]CVGI Discovery iMED, AstraZeneca, Macclesfield, SK10 4TG, UK,

Running title: Carnitine depletion alters fuel metabolism

Key Words: carnitine, muscle fuel selection, fat and carbohydrate metabolism

[†]Joint first author

***Corresponding author:**

Dumitru Constantin-Teodosiu, PhD

Phone: +44-115-8230111

Fax: +44-115-8230142

Email: tim.constantin@nottingham.ac.uk

This is an Accepted Article that has been peer-reviewed and approved for publication in the The Journal of Physiology, but has yet to undergo copy-editing and proof correction. Please cite this article as an 'Accepted Article'; doi: 10.1113/JP274415.

Table of Contents category: Muscle

Key points

Mildronate inhibits endogenous carnitine synthesis and tissue uptake, and accelerates urinary carnitine excretion, but the impact of mildronate mediated muscle carnitine depletion on whole-body fuel selection, and muscle fuel metabolism and its molecular regulation is under-investigated.

Ten days of oral mildronate administration did not impact on food or fluid intake, physical activity levels or body weight gain in the rat, but depleted muscle carnitine content (all moieties), increased whole-body carbohydrate oxidation and muscle and liver glycogen utilisation, and reduced whole-body fat oxidation.

Mildronate reduced carnitine transporter protein expression across muscles of different contractile and metabolic phenotypes. A TaqMan PCR low-density array card approach revealed the abundance of 189 mRNAs regulating fuel selection was altered in soleus muscle by mildronate; highlighting modulation of discrete cellular functions and metabolic pathways.

These novel findings strongly support the premise that muscle carnitine availability is a primary regulator of fuel selection *in vivo*.

Abstract

The body carnitine pool is primarily confined to skeletal muscle, where it regulates carbohydrate (CHO) and fat usage. Mildronate (3-(2,2,2-trimethylhydrazinium)-propionate) inhibits carnitine synthesis and tissue uptake, but the impact of carnitine depletion on whole-body fuel selection, muscle fuel metabolism and its molecular regulation is under-investigated. Male lean Zucker rats received water (control, *n=8*) or mildronate-supplemented water (mildronate, *n=8*) for 10 days (1.6 g·kg^{-1} body mass (bm)·day^{-1} day 1-2, 0.8 g·kg^{-1} bm·day^{-1} thereafter). From day 7-10, animals were housed in indirect calorimetry chambers after which soleus muscle and liver were harvested. Food and fluid intake, weight gain and physical activity levels were similar between groups from day 7-10. Compared to control, mildronate depleted muscle total carnitine (P<0.001) and all carnitine esters. Furthermore, whole-body fat oxidation was less (P<0.001) and CHO oxidation was greater (P<0.05) compared to control, whilst soleus and liver glycogen content were less (P<0.01 and P<0.01, respectively).

In a second study, male Wistar rats received water (n=8) or mildronate-supplemented water (n=8) as above, and kidney, heart, and EDL and soleus muscles were collected. Compared to control, mildronate depleted total carnitine content (all P<0.001), reduced carnitine transporter protein and glycogen content, and increased PDK4 mRNA abundance in heart, EDL, and soleus. 189 mRNAs regulating fuel selection were differentially expressed in soleus in mildronate vs control, and a number of cellular functions and pathways strongly associated with carnitine depletion were identified. Collectively, these data firmly support the premise that muscle carnitine availability is a primary regulator of fuel selection *in vivo*.

Abbreviations: Mildronate, (3-(2,2,2-trimethylhydrazinium)-propionate); PDK4, pyruvate dehydrogenase complex isoform 4; OCTN2, organic cation/carnitine transporter 2; CPT-1B, carnitine palmitoyl transferase 1; EDL, extensor digitorum longus muscle; IPA, Ingenuity Pathway Analysis; YWHAZ, tyrosine 3-Monooxygenase/Tryptophan 5-Monooxygenase Activation Protein; AMPK,AMP-activated protein kinase; PXR/RXR, the pregnane X receptor; CoASH, Coenzyme A; PDC, pyruvate dehydrogenase complex; CHO, carbohydrates

Introduction

Carnitine synthesis occurs mainly in the liver, but its storage is localised almost exclusively to the skeletal muscle (>90%) where it is involved in two discreet metabolic functions (Stephens *et al.*, 2007). Carnitine acts as an acetyl group buffer when the rate of oxidative carbohydrate (CHO) derived pyruvate decarboxylation to acetyl-CoA, which is controlled by the mitochondrial pyruvate dehydrogenase complex, exceeds the rate of acetyl-CoA utilisation in the tricarboxylic acid cycle (Harris *et al.*, 1987; Constantin-Teodosiu *et al.*, 1991a). Carnitine also plays a mandatory role in translocating cytosolic fatty acid derived long-chain acyl-CoAs across the otherwise impermeable inner mitochondrial membrane (Fritz & McEwen, 1959; Fritz & Yue, 1963). Furthermore, more recent evidence from studies in which muscle carnitine availability has been increased via insulin-mediated stimulation of muscle carnitine accumulation (Stephens *et al.*, 2006; Wall *et al.*, 2011; Stephens *et al.*, 2013) or pharmacologically depleted (Spaniol *et al.*, 2001) suggests that carnitine availability *per se* is a key regulator of muscle fuel selection. In short, a 20% increase in muscle carnitine content in young, healthy volunteers modulated changes in whole-body energy expenditure and quadriceps muscle fuel metabolism and gene expression entirely consistent with a carnitine-mediated increase in muscle fat oxidation as a consequence of increased muscle long-chain acyl-group translocation via CPT1

(Stephens *et al.*, 2006; Wall *et al.*, 2011; Stephens *et al.*, 2013). Conversely, it has also been proposed that the decline in muscle free carnitine availability that occurs in parallel with increasing exercise intensity (as a result of its acetylation by increased PDC flux) will ultimately limit CPT1 flux and thereby muscle fat oxidation (van Loon *et al.*, 2001). In keeping with this, the upsurge in muscle glycolytic and PDC flux that occurs during exercise as a consequence of increasing muscle glycogen availability prior to exercise, has been proposed to result in greater acetylation of muscle free carnitine leading to a reduction in long-chain fatty acid oxidation (Roepstorff *et al.*, 2005).

Despite its significance, little information is available concerning the impact of reduced muscle total carnitine content on fuel selection *in vivo*. Mildronate **(**3-(2,2,2-trimethylhydrazinium)-propionate), a γ-butyrobetaine (carnitine precursor) analogue, has been shown to: (i) impair liver carnitine biogenesis (Simkhovich *et al.*, 1988; Spaniol *et al.*, 2001); (ii) accelerate urinary free carnitine excretion (Kuwajima *et al.*, 1999; Spaniol *et al.*, 2001); (iii) reduce muscle carnitine transport *in vitro* (Georges *et al.*, 2000; Grigat *et al.*, 2009); (iv) reduce muscle carnitine availability and whole-body palmitate oxidation *in vivo* (Spaniol *et al.* 2001). More than 90% of the body carnitine pool is restricted to skeletal muscle, but to the best of our knowledge no research has collectively quantified the impact of mildronate administration on muscle carnitine content, daily energy and fluid intake, physical activity levels and whole-body fuel selection and muscle energy metabolism.

Skeletal muscle is composed of fibre types differing in their contractile and metabolic properties. We have previously shown no differences in the content of carnitine moieties between fibre types in human vastus lateralis muscle at rest (Constantin-Teodosiu *et al.*, 1996). However, the magnitude of carnitine acylation in human skeletal muscle during prolonged submaximal exercise was markedly greater in type I compared to type II fibres, supporting the

concept of fibre type-specific functional roles for carnitine in skeletal muscle connected to acetyl group buffering and mitochondrial long-chain acyl-CoA translocation, which will change depending on exercise intensity (Constantin-Teodosiu *et al.*, 1996). Although mildronate-mediated carnitine depletion has been reported in mixed-fibred rodent gastrocnemius (Tsoko *et al.*, 1995) and quadriceps femoris (Spaniol *et al.*, 2001) muscles, little is known regarding its relative impact on muscles of widely different metabolic and physiological characteristics, particularly from the same animal. Roberts et al. (Roberts *et al.*, 2015) reported that compared to control, mildronate mediated carnitine depletion was associated with reduced tension development and increased glycogen hydrolysis over 5 min of fatiguing contraction in muscle composed of predominantly Type II fibres (extensor digitorum longus, EDL). This contrasted the response seen in the slow contracting soleus muscle where contractile function and energy metabolism during contraction were apparently unaffected compared to control.

In the context of this background, our first aim was to test the hypothesis that compared to control, daily mildronate administration would have no impact on daily energy and fluid intake or physical activity levels *in vivo* in the rat. However, given the reciprocal relationship between lipid and CHO oxidation, it was also hypothesised that mildronate administration would attenuate whole-body fat oxidation compared with control animals as a result of depleting tissue carnitine stores, whilst concomitantly increasing whole-body CHO oxidation and reducing muscle and liver glycogen availability. A further aim was to highlight potential mechanisms by which mildronate-mediated carnitine depletion may have such metabolic effects, by specifically targeting for analysis genes and proteins thought to control carnitine linked-cellular fuel metabolism (e.g. carnitine transporter (OCTN2), pyruvate dehydrogenase kinase 4 (PDK4; carbohydrate oxidation), and carnitine palmitoyltransferase-1 (CPT1; fat oxidation), along with aspects of intermediary metabolism. Moreover, these analyses were performed in muscles of different contractile and metabolic phenotypes (heart, soleus and EDL muscles) to determine

fibre specific effects of mildronate-mediated carnitine depletion. Our final aim was to identify changes in cellular functions and metabolic pathways resulting from mildronate-induced carnitine depletion in soleus muscle (using low-density microarray cards and Ingenuity Pathway Analysis (IPA)), thereby providing novel insight of genes, cellular functions and metabolic pathways underpinning the comprehensive switch in fuel selection we hypothesised would be seen at a muscle and whole body level in mildronate vs control animals.

Materials and methods

Two studies were performed to test the stated aims and hypotheses. The first was conducted at AstraZeneca Pharmaceuticals, Alderley Park site, UK where whole-animal open circuit indirect calorimetry facilities were available, and the second in the animal research facility of the Biomedical Services Unit, University of Nottingham, UK. All tissue analyses were performed at the University of Nottingham. Both studies were approved by a local ethical review committee and had UK Home Office approval. All procedures were carried out in accordance with the Animals Scientific Act (1986). All animals were given free access to drinking water and standard chow throughout the study unless otherwise stated and body mass and fluid intake were monitored daily.

Study 1: The impact of mildronate administration on muscle carnitine content, whole-body fuel oxidation, muscle and liver glycogen availability, daily energy and fluid intake and physical activity levels *in vivo* in the rat

Sixteen male, lean Zucker rats (AstraZeneca Pharmaceuticals, Alderley Park colony), mean body weight 283 ± 6 g, were singly housed in standard cages in temperature and humidity controlled animal holding rooms at AstraZeneca Pharmaceuticals, Alderley Park, UK. Following a 7-day

period of acclimatisation, animals were randomly assigned to either control (*n=8*) or mildronate (*n=8*) treatment group. The control group received standard drinking water for 10 days, whilst the mildronate group received mildronate (Shandong Bangda Pharmaceutical Co, Ltd, China) supplemented drinking water over the same time period (priming dose of 1.6 $g \cdot kg^{-1}$ body mass (bm)$\cdot day^{-1}$ on days 1-2, followed by 0.8 $g \cdot kg^{-1}$ bm$\cdot day^{-1}$ thereafter). Mildronate solutions were prepared daily and the concentration prepared was based on an animal's body weight and fluid intake, which were monitored daily for 1 week before the study commenced. A similar dosing protocol was shown to result in a 13-fold reduction in hepatic carnitine content in Wistar rats (Degrace *et al.*, 2007), but we used a priming dose to ensure a steady-state blood mildronate concentration was be reached relatively quickly.

From days 7 to 10, control and mildronate treated animals were housed in Oxymax™ (Columbus Instruments, USA) open circuit indirect calorimetry cages equipped with the Comprehensive Laboratory Animal Monitoring System (CLAMS), which allowed continuous measurement of O_2 consumption (VO_2) and CO_2 production (VCO_2). In addition, food hoppers and volumetric drinkers allowed precise measurement of feeding and drinking behaviour and total daily dietary intake. The CLAMS system was also configured to measure tri-axis physical activity levels using a Columbus Instruments Opto-M3™ activity monitor. Each chamber was fitted with two rows of infra-red beams. Physical activity was scored as either single beam breaks or consecutive beam breaks representing ambulation, thereby allowing differentiation between rearing, grooming and ambulatory related physical activity. Grooming and ambulatory related activity were summed in order to calculate total activity. These measures allowed the differentiation between metabolic and physical activity-related changes in VO_2 and VCO_2 occurring as a result of any reduction in muscle carnitine content.

Fat and CHO oxidation rates were calculated from rates of VO_2 and VCO_2 according to equations previously described (Frayn, 1983). As urinary nitrogen excretion was not measured in this study, fat and CHO oxidation data are not presented as non-protein rates of substrate oxidation. Animals were allowed to acclimatise to the metabolic cages over the course of days 7 to 10 to ensure metabolic stability, and for the final 12 hr period were fasted to circumvent confounding effects of between-group differences in food intake on metabolic rate and patterns of substrate oxidation over this 12 hr period.

On the morning day 10 of the study following this 12 hr measurement period, animals were terminally anaesthetised with sodium thiobutabarbital (125 $mg \cdot kg^{-1}$ i.p. Inactin™, Sigma-Aldrich). The soleus muscle from each hind limb and a portion of the lateral hepatic lobe were then excised while still blood-perfused *in situ* and immediately (<5 s) submerged in liquid nitrogen.

Study 2: Mechanistic insight of the impact of mildronate mediated carnitine depletion on tissue fuel metabolism

Sixteen male Wistar rats (Charles River, Margate, UK), mean body weight 309 ± 5 g, were housed in pairs in standard cages in temperature and humidity controlled animal holding rooms in the Biomedical Services Unit at the University of Nottingham. Following acclimatisation to the experimental conditions, animals were randomly divided into 2 experimental groups that received the same interventions as described for Study 1 above, i.e. either standard drinking water (control, *n*=8), or drinking water supplemented with mildronate (mildronate, *n*=8) for 10 days (1.6 $g \cdot kg^{-1}$ $bm \cdot day^{-1}$ for 2 days and 0.8 $g \cdot kg^{-1}$ $bm \cdot day^{-1}$ thereafter). Mildronate solutions were prepared daily. After 10 days (i.e. morning of day 10), the EDL and soleus muscles of each hindlimb, along with the heart and a kidney, were harvested under terminal anaesthesia

(sodium pentobarbital, 120 mg kg^{-1} i.p. Sagatal, Rhone Merieux, UK), and snap-frozen in liquid nitrogen within 5 s of collection.

Metabolite measurements in soleus and liver (Study 1) and heart, extensor digitorum longus and soleus (Study 2)

Frozen tissue muscle samples were crushed under liquid nitrogen and a homogenate of wet tissue was freeze-dried for 24 hr. All visible blood and connective tissue were removed before each sample was powdered with forceps and a pestle and mortar. Metabolites were extracted from 6-10 mg of tissue powder in 0.5 mmol l^{-1} perchloric acid (PCA, containing 1 mmol l^{-1} EDTA) and following centrifugation, the extracts were neutralised with 2.2 mmol l^{-1} $KHCO_3$. In order to determine long-chain acylcarnitine content, the acid insoluble tissue pellet was re-suspended in 0.2 mmol l^{-1} KOH to alkali hydrolyse acylcarnitine bonds at 50° C for 2 hr before neutralisation with 5 mmol l^{-1} perchloric acid. Tissue free, long-chain acylcarnitine and acetylcarnitine content were subsequently determined using radio-enzymatic methods previously described (Cederblad & Lindstedt, 1972; Cederblad *et al.*, 1990). "Free carnitine and carnitine esters in order to calculate tissue total carnitine content. In addition, approximately 2 mg of powdered tissue was alkali-extracted in 0.1 M NaOH to determine tissue glycogen content spectrophotometrically as described previously (Harris *et al.*, 1974). In Study 2, the neutralised PCA extracts were also used to determine muscle ATP and PCr content using a modified spectrophotometric version of the method of Harris et al. (Harris *et al.*, 1974) to accommodate the use of a plate reader.

Targeted mRNA expression measurements in extensor digitorum longus, soleus and heart in Study 2

Total RNA was extracted from approximately 25 mg of EDL, soleus and heart muscle using Tri Reagent (Sigma-Aldrich, Poole, UK), and subsequently quantified spectrophotometrically at 260 nm with RNA purity being determined as the ratio of 260/280 nm readings. Thereafter, first strand cDNA synthesis was carried out according to methodology previously described (Constantin *et al.*, 2007). OCTN2, pyruvate dehydrogenase kinase 4 (PDK 4) and CPT1 transcripts were quantified by TaqMan PCR using an ABI prism 7000 sequence detector (Applied Biosystems, USA), with 2 µl of cDNA, 18 µM of each primer, and 5 µM probe and Universal TaqMan 2x PCR Mastermix (Eurogentec). Each sample was run in duplicate. Primers and MGB TaqMan probes (Applied Biosystems) are designed such that probes span over exon-exon boundaries to avoid genomic amplification. Hydroxymethylbilane synthase (HMBS) was used as internal control, and all genes of interest were labelled with the fluorescent reporter 5-FAM (5-Carboxyfluorescein). The thermal cycling conditions used were: 2 min at 50°C, 10 min at 95°C, followed by 40 cycles at 95°C for 15 s and 60°C for 1 min.

Soleus muscle mRNA expression levels using TaqMan low-density microarray cards in Study 2

Multiple mRNA expression measurements were made according to the manufacturer's instructions on 100 ng of cDNA obtained from total mRNA isolated from the soleus muscle collected from 7 animals in each treatment group using Applied Biosystems 384-well microfluidics TaqMan array cards (format 192 duplicates). The genes investigated were deemed to be representative of CHO, fat and cellular energy metabolism according to a search of the literature, and SA Biosciences and IPA databases. The Ct values generated by the Applied

Biosystems 7900HT Fast-Real Time PCR system were analysed and normalised to the geometric mean of the β-microglobulin and tyrosine 3-monooxygenase/tryptophan 5-monooxygenase activation protein (YWHAZ) mRNA expression values using Real-Time StatMiner (Integromics, Granada, Spain) software before being uploaded in Ingenuity Pathway Analysis (IPA) software (Redwood City, CA, USA) for pathway analysis of gene expression data. Ingenuity Pathway Analysis is a web-based commercial software application that enables analysis, integration, and understanding of data from gene expression, miRNA, and SNP microarrays, as well as metabolomics, proteomics, and RNAseq experiments. It can also be used for analysis of small-scale experiments that generate gene and chemical lists. Data analysis and interpretation with IPA builds on the comprehensive, manually curated content of the Ingenuity Knowledge Base. Powerful algorithms identify regulators, relationships, mechanisms, functions, and pathways relevant to changes observed in an analysed dataset. Analytics go beyond pathway analysis to understand experimental results within the context of biological systems (https://www.qiagen.com/ie/products/life-science-research/research-applications/gene-expression-analysis/analysis/ingenuity-pathway-analysis/).

Carnitine transporter (OCTN2) protein expression in Study 2

Samples of EDL, soleus, heart and kidney (positive control) were lysed in the presence of phosphatase and protease inhibitors and protein content was quantitated using a Bradford assay. Protein lysates were run on a 4-12% Bis-Tris acrylamide gel (Invitrogen, UK) for 2 hrs at constant voltage (200 V) and transferred to a polyvinylidene difluoride membrane (PVDF) overnight at constant 100 mA, in ice-cold buffers (4◦ C) as described by Constantin (Constantin *et al.*, 2007). The protein transfer was checked using Ponceau S red staining, before blocking the membrane in BSA-Tris buffer saline-tween (TBS-T) for 1 hr at room temperature. The

membranes were then probed with the primary antibodies against OCTN2 (Santa Cruz, CA, USA) and the endogenous α-actin (Sigma-Aldrich, St Louis, MO, USA) overnight at 4° C. The following day, membranes were washed in TBS-T, incubated with an IRDye 800 labelled anti-goat secondary antibody and further quantitated by using an Odyssey® Infrared Imaging System (LI-COR, Biosciences, NE, USA).

Statistical and Bioinformatics analysis

All values are presented as mean ± SEM unless otherwise stated. Comparison of mean values between treatment groups was performed using Student's unpaired *t*-test, one-way or two-way ANOVA with *Bonferroni* post hoc test analysis where appropriate (GraphPad Prism version 4, GraphPad software, San Diego, CA). For individual mRNA expression data depicted in Fig. 4, the fold-change difference in gene expression in the mildronate group relative to control was calculated with the $2^{-\Delta\Delta Ct}$ method, and an independent 2-group Mann-Whitney U Test was used to identify between-group differences. In all cases, statistical significance was accepted at $P<0.05$.

StatMiner software was used to generate a hierarchical clustering heat map (Fig. 6), depicting soleus muscle mRNA expression in the form of colours relative to housekeeping mRNAs (β-microglobulin and YWHAZ) for individual animals in each experimental group. This was done using Z-score normalisation, Ward's method for clustering and Euclidian distance as a similarity measurement. The following selection criteria were used: calibrator group = control; selected target = mildronate; adjustment method for false discovery rate (FDR) = Benjamin-Hochberg with the adjusted p-value threshold set at 0.05; the relative quantification visualisation scale = logarithmic. Regarding the Z-score normalization,

expression values in the hierarchical clustering were calculated as: x[i,j] z-score-normalized = (x[i,j] - mean[i]) / stdv[i]. Data in each row is centred on zero, as the mean was subtracted from all values, and the results were divided by the standard deviation, to prevent those rows with little variation losing contrast.

Differences in cellular functions from control associated with mildronate administration are depicted in Fig. 8. This was produced by IPA, utilising soleus muscle mRNA expression data generated using microfluidic TaqMan array cards. The x-axis displays cellular functions most affected by mildronate administration, while the y-axis displays the -log of the *p*-values. The *p*-value associated with each cellular function is a measurement of the likelihood that the association between a set of focus transcripts and a given function is due to random chance. The -log of *p*-value was calculated using Fisher's exact test (right-tailed).

Metabolic pathways different from control in mildronate treated animals is shown in Fig. 9. Again, this was produced by IPA utilising soleus muscle mRNA expression data generated using microfluidic TaqMan array cards. The x-axis displays those pathways most different from control following mildronate administration. The y-axis on the left displays the -log of the *p*-value for any given metabolic pathway. This was calculated by considering the number of measured transcripts that contributed to that pathway and the total number of transcripts known to be associated with that pathway in Ingenuity's knowledge base. The -log of p-value was calculated using Fisher's exact test (right-tailed). The threshold was set at $P<0.05$. The y-axis on the right depicts the ratio of the number of genes in a given pathway that meet cut-off criteria ($P<0.05$), divided by the total number of genes that make up that pathway.

Results

Study 1: The impact of mildronate administration on muscle carnitine content, whole-body fuel oxidation, muscle and liver glycogen availability, daily energy and fluid intake and physical activity levels *in vivo* in the rat

Food and fluid intake, physical activity levels and body mass

Daily food intake (20.5±0.4 g·day^{-1} vs 19.3±0.6 g·day^{-1}), fluid intake (32.3±0.9 ml·day^{-1} vs 38.4±1.5 ml·day^{-1}) and physical activity levels (10,305±875 vs 9,219±588 scores·day^{-1}) were no different between control and mildronate treated groups, respectively, over the 3 days (days 7 to 10) animals were housed in indirect calorimetry cages equipped with CLAMS. Furthermore, mildronate had no effect on body mass gains during the 10 day study period compared with control, i.e. control animals gained 6.2±1.2 g in body mass, and mildronate treated animals gained 5.9±2.0 g.

Metabolite measurements in soleus and liver

Soleus muscle carnitine esters in control and mildronate treated groups at the end of the 10 day study period are presented in Table 1. Mildronate treated animals had markedly less muscle free (90%, P<0.001), acyl (65%, P<0.05), acetyl (51%, P<0.05) and total (80%, P<0.001) carnitine content compared to control. In addition, muscle and liver glycogen content in the mildronate group was less than in control (22.4±2.6 vs 37.4±4.0 mmol·kg^{-1} dm, P<0.01 and 6.0±1.9 vs 22.1±3.8 mmol·kg^{-1} dm, P<0.01 respectively; Figure 1).

Whole-body fuel oxidation

The rate of whole-body fat oxidation on day 10 over the 12 hr period during which animals were fasted is presented in Figure 2. The rate of fat oxidation in the mildronate treated group was significantly less than control throughout (P<0.001, Figure 2A), such that total fat oxidation was 19% less in mildronate than control (7,027±123 vs 5,647±127 μmol·kg^{-1} bm, P<0.001; Figure 2B). Conversely, and in keeping with the muscle and liver glycogen responses reported (Figure 1), the rate of CHO oxidation in the mildronate treated group over the initial 2 hr period was greater than in control (P<0.05, Figure 3A), resulting in total CHO oxidation over the 12 hr period being 16% greater in mildronate (3,617±155 vs 4,191±202 μmol·kg^{-1} bm, P<0.05; Figure 3B).

Study 2: Mechanistic insight of the potential impact of mildronate mediated carnitine depletion on tissue fuel metabolism

Food and fluid intake, physical activity levels and body mass

Mildronate supplementation had no impact on daily food or water consumption when compared to control. Mildronate administration did not affect body mass over the course of the study. The average mass gain was 70 ± 3 g in the control group compared with 68 ± 3 g in the mildronate group.

Metabolite measurements in the heart, extensor digitorum longus and soleus muscle

Tissue free carnitine content and carnitine esters are presented in Table 2. Free carnitine content was noticeably less in all tissues from mildronate treated animals when compared with control (by 90%, P<0.001; 86%, P<0.001; and 84%, P<0.001 in heart, EDL, and soleus; respectively). Long-chain acylcarnitine content was also markedly less in heart, EDL and soleus

of mildronate treated animals compared with control (by 72%, $P<0.001$; 64%, $P<0.01$; and 31%; $P<0.05$, respectively), as was the acetylcarnitine content in heart (39%, $P<0.05$), EDL (55%, $P<0.05$), and soleus (25%, $P<0.05$). As expected from these observations, muscle total carnitine content was less in all tissues from mildronate treated animals compared to control (by 81%, $P<0.001$; 81%, $P<0.001$; and 73%, $P<0.001$, in heart, EDL, and soleus; respectively).

Tissue ATP, PCr and glycogen content is presented in Table 3. No differences in ATP or PCr content were observed when comparing carnitine-depleted and control animals. Glycogen content was less in heart, EDL and soleus in the carnitine-depleted animals compared with control (29%, $P<0.05$, 26%, $P<0.05$ and 26%, $P<0.05$; respectively).

Targeted mRNA expression in the heart, extensor digitorum longus and soleus muscle

OCTN2, CPT-1B and PDK4 mRNA expression in heart, EDL and soleus muscle from control and mildronate treated animals is shown in Fig. 4. OCTN2 mRNA expression was greater in heart from mildronate treated animals compared with control (1.9-fold, $P<0.05$), but not in EDL and soleus. Expression of CPT-1 mRNA in heart and EDL was no different between treatment groups, but its expression was greater in soleus of midronate treated animals (2.1-fold, $P<0.001$). PDK4 mRNA expression was greater than control in heart (4.5-fold, $P<0.001$), EDL (2.2-fold, $P<0.001$) and the soleus (2.2-fold, $P<0.001$) from mildronate treated animals.

OCTN2 protein expression

Carnitine transporter protein expression, and representative Western blots of OCTN2 protein detected at 63 kDa, is presented in Fig. 5A and B, respectively. OCTN2 protein expression in heart, soleus, EDL and kidney (the latter used as a positive internal control because of its high OCTN2 expression (Tamai *et al.*, 1998) was less in mildronate treated animals than control (78%, $P<0.001$; 54%, $P<0.05$; 56%, $P<0.05$; 36%, $P<0.05$; respectively).

Soleus muscle mRNA expression levels using TaqMan low-density microarray cards

Figure 6 depicts a hierarchical clustering heat map illustrating relative soleus muscle mRNA expression in individual animals of the two treatment groups (data were normalised to the geometric mean of the housekeeping genes β-microglobulin and YWHAZ (tyrosine 3-Monooxygenase/Tryptophan 5-Monooxygenase Activation Protein) for all 189 transcripts investigated, see Materials and methods). The figure illustrates that whilst between animal variation was present, a pattern of between treatment group divergence was also apparent, such that soleus muscle mRNA expression in mildronate treated animals was generally greater (red) relative to housekeeping genes, compared to control animals where generally less mRNA expression relative to the same housekeeping genes was observed (green). Overall, 158 transcripts were up-regulated and 31 transcripts were downregulated in mildronate treated animals compared to control (-2.6 ≤ range ≤3.3-fold change). Figure 7 shows that of those genes up-regulated in mildronate treated animals compared to control, insulin receptor (INSR), C2-12 straight-chain Acyl-CoA dehydrogenase (ACADM), acetyl-CoA carboxylase (MLYCD), hydroxysteroid (17-β) dehydrogenase (HSD17B4), and to a lesser extent PDK4 (pyruvate dehydrogenase isoform 4), carnitine palmitoyl-transferase 2 (CTP2) Akt1 and IL-6, were the most notably affected. Of those genes down-regulated in mildronate relative to control, FOXO1, peroxisome proliferator-activated receptor α, δ, γ, peroxisome proliferator-activated receptor gamma, co-activator 1α (PPARGC1A), transforming growth factor, β (TGFB1), and to a lesser extent carnitine transporter (SLC22A5) and sterol regulatory element binding transcription factor 1 (SREBF1), were the most affected (Fig. 7). Based on the collective differences in mRNA expression between mildronate and control animals, IPA predicted a comprehensive inhibition of soleus muscle fat oxidation, and particularly long-chain fatty acid and palmitic acid oxidation, along with a prediction of an increase in glucose oxidation, albeit to a lesser extent (Fig. 7).

Another way to consider the data is highlighted in Fig. 8, which shows predicted changes in cellular functions as a result of mildronate administration generated by IPA (using the soleus mRNA expression from the TaqMan array cards). Here, and in keeping with Fig. 7, the most noticeably affected cellular functions associated with mildronate administration were energy production, lipid metabolism, and CHO metabolism (-log (*p*-value) ≥30). Figure 9 highlights those metabolic pathways most different from control (up or down) in mildronate treated animals, and which most likely underpin the shifts in cellular functions predicted in Fig. 8. AMPK signalling, glycolysis, nuclear receptor PXR/RXR activation, insulin receptor signalling, PPARα activation and fatty acid beta-oxidation were the most obviously affected (-log (*p*-value)>5).

Discussion

Carnitine plays well-documented roles in muscle energy metabolism, and the ability to alter the muscle carnitine pool is central to furthering our understanding of the role of carnitine availability in the regulation of muscle fuel selection. Several studies have investigated the impact of increasing muscle carnitine availability on muscle energy metabolism in humans (Stephens *et al.*, 2006; Wall *et al.*, 2011; Stephens *et al.*, 2013), but little is known about the metabolic consequences of muscle carnitine depletion. Mildronate is thought to inhibit hepatic carnitine biogenesis, tissue carnitine transport and renal carnitine retention (Spaniol *et al.*, 2001). Here, we demonstrate that 10 days of oral mildronate administration was associated with markedly lower muscle carnitine content relative to control (an effect seen across all carnitine esters and in several muscle phenotypes in two independent experiments). Moreover, this was paralleled by lower rates of whole-body fat oxidation relative to control animals, and in keeping with this, greater rates of whole-body CHO oxidation, and muscle and liver glycogen

depletion. Mildronate did not impact upon daily energy or fluid intake, habitual physical activity levels or body mass gains. Collectively, these novel findings support the premise that muscle carnitine availability is a primary regulator of muscle fuel selection *in vivo*.

Although carnitine is the primary substrate for the carnitine transporter OCTN2, it is known that efficacy of transmembrane transport of mildronate by OCTN2 is greater than that of carnitine (Grigat et. 2009). Moreover, administration of mildronate to rodents *in vivo* increased urinary free carnitine excretion by 30-fold (Kuwajima *et al.*, 1999; Spaniol *et al.*, 2001). In the present study, 10 days mildronate treatment resulted in substantial differences in muscle total carnitine content compared to control in two rodent species, which is consistent with the observations of others (Spaniol *et al.*, 2001; Roberts *et al.*, 2015). Furthermore, we demonstrated this effect was distributed across all muscle carnitine esters, and in heart and muscles of widely different metabolic phenotypes (Table 1 and 2). Of importance, this mildronate mediated carnitine depletion was accompanied by less expression of carnitine transporter protein (OCTN2) in all tissues relative to control (Fig. 5). Heart, in particular, showed the most marked (70%) difference in OCTN2 protein expression from control, which was paralleled by greater OCTN2 mRNA expression (1.9-fold) relative to control (not evident in skeletal muscle), pointing to the induction of a transcriptional response to restore carnitine transporter protein in this tissue. It appears therefore that OCTN2 mRNA and protein expression levels in the heart are more tightly regulated by carnitine availability than in muscle. Indeed, given heart carnitine content can be acutely increased by dietary or i.v. carnitine administration (Bartels *et al.*, 1992), which is not the case for skeletal muscle (Stephens *et al.*, 2006), this also supports the suggestion that heart tissue exhibits greater sensitivity to acute changes in plasma and tissue carnitine availability. The present observations are also consistent with the report that mildronate does not affect OCTN2 mRNA expression in mixed-fibre skeletal muscles (quadriceps femoris; (Schurch *et al.*, 2010), suggesting muscle OCTN2 transcription

does not respond to acute plasma and tissue carnitine depletion, or to increased OCTN2 substrates, such as mildronate and γ-butyrobetaine, which are elevated in the plasma as a consequence of mildronate administration (Liepinsh *et al.*, 2006; Liepinsh *et al.*, 2011b). However, under conditions of chronically reduced plasma and muscle carnitine availability, as occurs in long-standing human vegetarianism, a decline in muscle OCTN2 protein expression can be expected in humans (Stephens *et al.*, 2011).

Although pharmacological carnitine depletion has been documented in gastrocnemius, quadriceps, soleus and EDL muscles, heart and liver (Tsoko *et al.*, 1995; Spaniol *et al.*, 2001; Liepinsh *et al.*, 2006; Degrace *et al.*, 2007; Liepinsh *et al.*, 2008; Liepinsh *et al.*, 2009a), the metabolic impact of muscle carnitine depletion on lipid and CHO oxidation remains under-investigated. Collectively, our observations strongly advocate that the mildronate mediated reduction in muscle free carnitine content observed was limiting to muscle CPT1 flux, as evidenced by the lower long-chain muscle acylcarnitine (end product of CPT1 reaction) content compared to control (Table 1 and 2), and ultimately the lower rate of whole-body fat oxidation in mildronate treated animals vs control (Fig. 2A and 2B). In line with our findings, Spaniol et al. (Spaniol *et al.*, 2001) reported that muscle carnitine content was reduced after 3 weeks of mildronate administration in the rat, whilst expired $^{14}CO_2$ following acute ^{14}C palmitate administration was also reduced. Spaniol et al. (2001) attributed this acute reduction in ^{14}C palmitate oxidation to a decline in hepatic fat oxidation. However, this could perhaps be expected given the palmitate tracer was administered i.p. Indeed, given that >90% of the body total carnitine pool is restricted to the skeletal muscle (Brass, 1995), it is likely that the major part of the change in tissue fuel selection was muscle specific. Indeed, *in vitro* experiments have reported the Michaelis-Menten constant (*Km*) of CPT1 for carnitine is 0.5 $mmol \cdot l^{-1}$ (McGarry *et al.*, 1983), and in the present study muscle free carnitine content in mildronate treated animals was 0.35±0.03 $mmol \cdot kg^{-1}dm$ (or <0.1 $mmol \cdot l^{-1}$ intracellular water), which is well below this

reported *Km* value and would have markedly reduced muscle CPT1 enzyme kinetics. Further evidence that muscle free carnitine depletion plays a key role in reducing CPT1 flux and regulating fuel selection comes from studies of patients with systemic carnitine deficiency, in whom muscle carnitine is depleted and the capacity to oxidise long-chain fatty acids is reduced (Engel & Angelini, 1973). The observation that both muscle long-chain acylcarnitine content and long-chain fatty acid oxidation are reduced under conditions of exercise-mediated carnitine acetylation in healthy volunteers also lends support to this premise (Sidossis *et al.*, 1996b; van Loon *et al.*, 2001; Rasmussen *et al.*, 2002). The current data also complement studies proposing that increasing, rather than decreasing, muscle carnitine availability increases lipid utilisation at rest and spares muscle glycogen use during low-intensity exercise (Stephens *et al.*, 2006; Wall *et al.*, 2011; Stephens *et al.*, 2013) in healthy, young volunteers.

The reduction in whole-body fat oxidation observed in mildronate mediated carnitine-depleted animals compared to control (Fig. 2) was accompanied by a concurrent increase in whole-body CHO oxidation (16% greater in the mildronate group compared to control, Fig. 3), and lower muscle and liver glycogen content (Fig. 1). This is not surprising given the well-documented reciprocal relationship between muscle fat and CHO oxidation (Randle *et al.*, 1963; Sidossis & Wolfe, 1996a). Interestingly, PDK4 mRNA expression was greater in heart, soleus and EDL muscles of mildronate treated animals relative to control (Fig. 4C), which we suggest could reflect an adaptive response aimed at inhibiting PDC activation and sparing CHO as a consequence of a carnitine depletion mediated increase in tissue CHO use. Indeed, muscle PDK4 mRNA expression has been reported to be increased under conditions of reduced muscle glycogen availability (exercise-mediated), which the authors proposed was attributable to glycogen availability *per se* up-regulating PDK4 transcription (Pilegaard *et al.*, 2002). Furthermore, we have previously reported that increased PDK4 mRNA expression is accompanied by an increase in PDK4 protein expression in rodents (Constantin *et al.*, 2007;

Crossland *et al.*, 2008; Crossland *et al.*, 2010) and in humans (Constantin *et al.*, 2011) under a variety of experimental conditions, which we have no reason to question did not occur in the present study. However, we acknowledge that since whole-body fat oxidation was lower in the mildronate treated animals compared with control that allosteric regulation of PDC could have also played a role in the increase in whole-body CHO oxidation and muscle glycogen use. Of note, unlike the effect on fat oxidation, the impact of muscle carnitine depletion on CHO oxidation dissipated over the 12 hr study period (Fig. 3A), such that CHO oxidation declined as body CHO stores became exhausted (evidenced by the very low muscle and liver glycogen content in the mildronate treated animals (Fig. 1, Table 2). This is more than likely attributable to the animals being fasted over this time, which was necessary to allow direct comparison of the whole body and tissue fuel utilisation between mildronate and control treated animals. In contrast to humans, where an overnight fast will have minimal impact on skeletal muscle glycogen stores (~ 400 $mmol \cdot kg^{-1}$ dry muscle), rodents are metabolically active reflected by a relatively high metabolic turnover requiring liver and muscle glycogen utilisation during fasting (Freminet & Leclerc, 1980); corroborated by the fasted state low liver and muscle glycogen levels even in the control animals of the present study (Fig. 1). Notably, mildronate treatment did not affect food intake, water consumption or physical activity levels over the 3 day period when animals were housed in the calorimetric chambers, demonstrating that the mildronate induced changes in whole-body fuel oxidation during the final 12 hr of the study, when animal access to food was removed, occurred independent of diet and/or habitual physical activity level related changes in energy metabolism.

An important objective of the current study was to identify changes in cellular functions and metabolic pathways from control as a result of mildronate induced carnitine depletion in the soleus muscle using low-density microarray cards and IPA. Based on fold changes in mRNA expression of 192 targeted transcripts (158 up-regulated and 31 down-regulated relative to

control), IPA predicted a comprehensive inhibition of fat oxidation in the soleus muscle, and particularly long-chain fatty acid and palmitic acid oxidation, along with an increase in glucose oxidation (Fig. 7). In keeping with this, the cellular functions most notably affected by carnitine depletion were energy production, lipid metabolism, and CHO metabolism (Fig. 8). Furthermore, IPA highlighted AMPK signalling, glycolysis, nuclear receptor PXR/RXR activation, insulin receptor signalling, PPARα activation and fatty acid beta-oxidation as being the most likely pathways mediating these changes in cellular functions (-log(*p*-valued) ≥30, Fig. 9). Although AMPK is accepted to be activated by a decrease in the cellular ATP/ADP ratio (Fimland *et al.*, 2010), we found no evidence of a mildronate mediated reduction in ATP or PCr (a highly sensitive marker of cellular energy status) content in any tissue investigated (Table 3). However, AMPK is also activated by several drugs and xenobiotics, including anti-diabetic drugs (such as metformin and rosiglitazone; (Fryer *et al.*, 2002), or more pertinent to the present study by low muscle glycogen availability (Richter & Ruderman, 2009). Of note, carnitine depletion markedly suppressed the expression of several PPARs (Fig. 7), which is in keeping with the observation that carnitine supplementation increases the level of muscle PPARα mRNA in human skeletal muscle (Stephens *et al.*, 2013). Our approach has therefore generated novel insight of mechanisms associated with the comprehensive differences in fuel use at a whole body and tissue level in mildronate treated animals vs control. Whether these mRNA expression differences occurred as a direct result of mildronate administration markedly reducing carnitine availability and/or indirectly as a result of a change in tissue fuel utilisation cannot be discerned from this study.

Carnitine depletion resulted in a 2-fold increase in CPT-1 mRNA expression in soleus, but not heart or EDL. While carnitine depletion has been reported to impair CPT-1 activity in the heart (Liepinsh *et al.*, 2009a), heart tissue is known to express both CPT-1A (hepatic) and CPT-1B (muscle) isoforms, whereas skeletal muscle expresses only CPT-1B. As the K_m of CPT-1B for

carnitine is approximately 60-fold greater than that of CPT-1A (McGarry *et al.*, 1983), this may explain why CPT-1 mRNA expression was increased in the soleus relative to control, particularly when considering that free carnitine was reduced to 0.47 mmol kg^{-1} dry muscle (~ 0.17 mmol l^{-1} intracellular water) in this muscle, which is well below the reported K_m of CPT-1 for carnitine (0.5 mmol l^{-1} ; Brass, 1995). In keeping with this, oxfenicine (a muscle-specific inhibitor of CTP-1B activity) has been associated with decreased fat oxidation and accumulation and increased CHO use in mouse gastrocnemius muscle (Keung *et al.*, 2012).

In summary, we have demonstrated that acute mildronate administration caused widespread and substantial tissue carnitine depletion *in vivo*, which was associated with reduced OCTN2 protein expression in heart, soleus and EDL muscles compared to control. Relative to control, carnitine depletion was also linked to lower glycogen content across these tissues of differing phenotype, and was accompanied by an increase in PDK4 mRNA expression in all tissues. Of further novelty, muscle carnitine depletion was associated with a lower rate of whole-body fat oxidation *in vivo* compared with control, and a concomitant greater rate of whole-body CHO oxidation, which was associated with lower muscle and liver glycogen contents in these animals. Further scrutiny identified a comprehensive difference in soleus muscle expression of mRNAs regulating a number of fuel selection regulatory pathways in mildronate vs control treated animals, which we propose was mechanistically linked to the differences seen in fuel oxidation and glycogen content between treatment groups. These findings complement reports documenting that an increase in human muscle carnitine content produces adaptive metabolic and genomic responses consistent with an increase in muscle lipid oxidation relative to control (Stephens *et al.*, 2013), and collectively they highlight a central role of muscle carnitine availability in the regulation of muscle fuel selection.

REFERENCES

Bartels GL, Remme WJ, Pillay M, Schonfeld DH, Cox PH, Kruijssen HA & Knufman NM. (1992). Acute improvement of cardiac function with intravenous L-propionylcarnitine in humans. *J Cardiovasc Pharm* **20,** 157-164.

Brass EP. (1995). Pharmacokinetic considerations for the therapeutic use of carnitine in hemodialysis patients. *Clin Ther* **17,** 176-185.

Cederblad G, Carlin J, Constantin-Teodosiu D, Harper P & Hultman E. (1990). Radioisotopic assays of CoASH and carnitine and their acetylated forms in human skeletal muscle. *Anal Biochem* **185,** 274-278.

Cederblad G & Lindstedt S. (1972). A method for the determination of carnitine in the picomole range. *Clin Chim Acta* **37,** 235-243.

Constantin-Teodosiu D, Carlin J, Cederblad G, Harris R & Hultman E. (1991a). Acetyl group accumulation and pyruvate dehydrogenase activity in human muscle during incremental exercise. *Acta Physiol Scand* **143,** 367-372.

Constantin-Teodosiu D, Howell S & Greenhaff P. (1996). Carnitine metabolism in human muscle fiber types during submaximal dynamic exercise. *J Appl Physiol* **80,** 1061-1064.

Constantin D, Constantin-Teodosiu D, Layfield R, Tsintzas K, Bennett A & Greenhaff PL. (2007). PPARdelta agonism induces a change in fuel metabolism and activation of an atrophy programme, but does not impair mitochondrial function in rat skeletal muscle. *J Physiol* **583,** 381-390.

Constantin D, McCullough J, Mahajan RP & Greenhaff PL. (2011). Novel events in the molecular regulation of muscle mass in critically ill patients. *J Physiol* **589,** 3883-3895.

Crossland H, Constantin-Teodosiu D, Gardiner SM, Constantin D & Greenhaff PL. (2008). A potential role for Akt/FOXO signalling in both protein loss and the impairment of muscle carbohydrate oxidation during sepsis in rodent skeletal muscle. *J Physiol* **586,** 5589-5600.

Crossland H, Constantin-Teodosiu D, Greenhaff PL & Gardiner SM. (2010). Low-dose dexamethasone prevents endotoxaemia-induced muscle protein loss and impairment of carbohydrate oxidation in rat skeletal muscle. *J Physiol* **588,** 1333-1347.

Degrace P, Demizieux L, Du Z, Gresti J, Caverot L, Djaouti L, Jourdan T, Moindrot B, Guilland J, Hocquette J & Clouet P. (2007). Regulation of lipid flux between liver and adipose tissue during transient hepatic steatosis in carnitine-depleted rats. *J Biol Chem* **20,** 20816-20826.

Engel A & Angelini C. (1973). Carnitine deficiency of human skeletal muscle with associated lipid storage myopathy: a new syndrome. *Science* **179,** 899-902.

Fimland MS, Helgerud J, Gruber M, Leivseth G & Hoff J. (2010). Enhanced neural drive after maximal strength training in multiple sclerosis patients. *Eur J Appl Physiol* **110,** 435-443.

Frayn K. (1983). Calculation of substrate oxidation rates in vivo from gaseous exchange. *J Appl Physiol* **55,** 628-634.

Freminet A & Leclerc L. (1980). Effect of fasting on liver and muscle glycogen in rats and guinea pigs. *J Physiol (Paris)* **76,** 877-880.

Fritz I & Yue K. (1963). Long chain carnitine acyl transferase and the role of acylcarnitines in the catalytic increase of fatty acid oxidation by carnitine. *J Lipid Res* **4,** 279-288.

Fritz IB & McEwen B. (1959). Effects of carnitine on fatty-acid oxidation by muscle. *Science* **6,** 334-335.

Fryer LG, Parbu-Patel A & Carling D. (2002). The Anti-diabetic drugs rosiglitazone and metformin stimulate AMP-activated protein kinase through distinct signaling pathways. *J Biol Chem* **277,** 25226-25232.

Georges B, Le Borgnea F, Gallanda, Isoira M, Ecossea D, Grand-Jeana F & Demarquoy J. (2000). Carnitine transport into muscular cells. inhibition of transport and cell growth by mildronate *Biochem Pharm* **59,** 1357-1363.

Grigat S, Fork C, Bach M, Golz S, Geerts A, Schömig E & Gründemann D. (2009). The carnitine transporter SLC22A5 is not a general drug transporter, but it efficiently translocates mildronate. *Drug Metab Dispos* **37,** 330-337.

Harris R, Foster C & Hultman E. (1987). Acetylcarnitine formation during intense muscular contraction in humans. *J Appl Physiol* **63,** 440-442.

Harris R, Hultman E & Nordesjö L. (1974). Glycogen, glycolytic intermediates and high-energy phosphates determined in biopsy samples of musculus quadriceps femoris of man at rest. Methods and variance of values. *Scand J Clin Lab Invest* **33,** 109-120.

Keung W, Ussher JR, Jaswal JS, Raubenheimer M, Lam VH, Wagg CS & Lopaschuk GD. (2012). Inhibition of Carnitine Palmitoyltransferase-1 Activity Alleviates Insulin Resistance in Diet-Induced Obese Mice. *Diabetes*.

Kuwajima M, Harashima H, Hayashi M, Saori I, Masako S, Kang-Mo L, Kiwada H, Sugiyama Y & Shima K. (1999). Pharmacokinetic analysis of the cardioprotective effect of 3-(2,2,2-trimethylhydrazinium) propionate in mice: Inhibition of carnitine transport in kidney. *J Pharm Exp Therap* **289,** 93-102.

Liepinsh E, Kuka J, Svalbe B, Vilskersts R, Skapare E, Cirule H, Pugovics O, Kalvinsh I & Dambrova M. (2009a). Effects of Long-Term Mildronate Treatment on Cardiac and Liver Functions in Rats. *Basic Clin Pharmacol Toxicol* **105,** 387-394.

Liepinsh E, Skapare E, Svalbe B, Makrecka M, Cirule H & Dambrova M. (2011b). Anti-diabetic effects of mildronate alone or in combination with metformin in obese Zucker rats. *Eur J Pharm* **658,** 277-283.

Liepinsh E, Vilskersts R, Loca D, Kirjanova O, Pugovichs O, Kalvinsh I & Dambrova M. (2006). Mildronate, an inhibitor of carnitine biosynthesis, induces an increase in gamma-butyrobetaine contents and cardioprotection in isolated rat heart infarction. *J Cardivasc Pharm* **48,** 314-319.

Liepinsh E, Vilskersts R, Skapare E, Svalbe B, Kuka J, Cirule H, Pugovics O, Kalvinsh I & Dambrova M. (2008). Mildronate decreases carnitine availability and up-regulates glucose uptake and related gene expression in the mouse heart. *Life sci* **83,** 613-619.

McGarry J, Mills S, Long C & Foster D. (1983). Observations on the affinity for carnitine, and malonyl-CoA sensitivity, of carnitine palmitoyltransferase I in animal and human tissues. Demonstration of the presence of malonyl-CoA in non-hepatic tissues of the rat. *Biochem J* **15,** 21-28.

Pilegaard H, Keller C, Steensberg A, Helge JW, Pedersen BK, Saltin B & Neufer PD. (2002). Influence of pre-exercise muscle glycogen content on exercise-induced transcriptional regulation of metabolic genes. *J Physiol* **541,** 261-271.

Randle P, Garland P, Hale C & Newsholme E. (1963). The glucose fatty-acid cycle. Its role in insulin sensitivity and the metabolic disturbances of diabetes mellitus. *Lancet* **1,** 785-789.

Rasmussen B, Holmbäck U, Volpi E, Morio-Liondore B, Paddon-Jones D & Wolfe R. (2002). Malonyl coenzyme A and the regulation of functional carnitine palmitoyltransferase-1 activity and fat oxidation in human skeletal muscle. *J Clin Invest* **110,** 1687-1693.

Richter EA & Ruderman NB. (2009). AMPK and the biochemistry of exercise: implications for human health and disease. *Biochem J* **418,** 261-275.

Roberts PA, Bouitbir J, Bonifacio A, Singh F, Kaufmann P, Urwyler A & Krahenbuhl S. (2015). Contractile function and energy metabolism of skeletal muscle in rats with secondary carnitine deficiency. *Am J Physiol Endo Metab* **309,** E265-274.

Roepstorff C, Halberg N, Hillig T, Saha AK, Ruderman NB, Wojtaszewski JF, Richter EA & Kiens B. (2005). Malonyl-CoA and carnitine in regulation of fat oxidation in human skeletal muscle during exercise. *Am J Physiol Endo Metab* **288,** 133-142.

Schurch R, Todesco L, Novakova K, Mevissen M, Stieger B & Krahenbuhl S. (2010). The plasma carnitine concentration regulates renal OCTN2 expression and carnitine transport in rats. *Eur J Pharm* **635,** 171-176.

Sidossis L, Stuart C, Shulman G, Lopaschuk G & Wolfe R. (1996b). Glucose plus insulin regulate fat oxidation by controlling the rate of fatty acid entry into the mitochondria. *J Clin Invest* **98,** 2244-2250.

Sidossis LS & Wolfe RR. (1996a). Glucose and insulin-induced inhibition of fatty acid oxidation: the glucose-fatty acid cycle reversed. *Am J Physiol Endo Metab* **270,** 733–738.

Simkhovich B, Shutenko Z, Meirena D, Khagi K, Mezapuķe R, Molodchina T, Kalviņs I & Lukevics E. (1988). 3-(2,2,2-Trimethylhydrazinium)propionate (THP)--a novel gamma-butyrobetaine hydroxylase inhibitor with cardioprotective properties. *Biochem Pharm* **15,** 195-202.

Spaniol M, Brooks H, Auer L, Zimmermann A, Solioz M, Stieger B & Krähenbühl S. (2001). Development and characterization of an animal model of carnitine deficiency. *Eur J Biochem* **268,** 1876–1887.

Stephens FB, Constantin-Teodosiu D, Laithwaite D, Simpson EJ & Greenhaff PL. (2006). An acute increase in skeletal muscle carnitine content alters fuel metabolism in resting human skeletal muscle. *J Clin Endo Metab* **91,** 5013-5018.

Stephens FB, Constantin-Teodosiu D & Greenhaff PL. (2007). New insights concerning the role of carnitine in the regulation of fuel metabolism in skeletal muscle. *J Physiol* **581,** 431-444.

Stephens FB, Marimuthu K, Cheng Y, Patel N, Constantin D, Simpson EJ & Greenhaff PL. (2011). Vegetarians have a reduced skeletal muscle carnitine transport capacity. *Am J Clin Nutr* **94,** 938-944.

Stephens FB, Wall BT, Marimuthu K, Shannon CE, Constantin-Teodosiu D, Macdonald IA & Greenhaff PL. (2013). Skeletal muscle carnitine loading increases energy expenditure, modulates fuel metabolism gene networks and prevents body fat accumulation in humans. *J Physiol* **591,** 4655-4666.

Tamai I, Ohashi R, Nezu J-i, Yabuuchi H, Oku A, Shimane M, Sai Y & Tsuji A. (1998). Molecular and Functional Identification of Sodium Ion-dependent, High Affinity Human Carnitine Transporter OCTN2. *J Biol Chem* **273,** 20378-20382.

Tsoko M, Beauseigneur F, Gresti J, Niot I, Demarquoy J, Boichot J, Bezard J, Rochette L & Clouet P. (1995). Enhancement of activities relative to fatty acid oxidation in the liver of rats depleted of L-carnitine by D-carnitine and a gamma-butyrobetaine hydroxylase inhibitor. *Biochem Pharm* **49,** 1403-1410.

van Loon LJ, Greenhaff PL, Constantin-Teodosiu D, Saris WH & Wagenmakers AJ. (2001). The effects of increasing exercise intensity on muscle fuel utilisation in humans. *J Physiol* **536,** 295–304.

Wall BT, Stephens FB, Constantin-Teodosiu D, Marimuthu K, Macdonald IA & Greenhaff PL. (2011). Chronic oral ingestion of L-carnitine and carbohydrate increases muscle

carnitine content and alters muscle fuel metabolism during exercise in humans. *J Physiol* **589,** 963-973.

Competing interests.

The authors declare they have no competing financial interests in relation to the work described here.

Author contributions

C.P. - Generation of experimental hypothesis and study design, research data, wrote and edited the manuscript

D.C.T. - Generation of experimental hypothesis and study design, research data, wrote and edited the manuscript.

D.C. - Research data, reviewed and edited the manuscript

B.L. - Reviewed and edited the manuscript

S.P. - Generation of experimental hypothesis and study design, reviewed and edited the manuscript

P.L.G. - Generation of experimental hypothesis and study design, wrote and edited the manuscript.

All authors: approved the final version of the manuscript; and agreed to be accountable for all aspects of the work in ensuring that questions related to the accuracy or integrity of any part of the work are appropriately investigated and resolved; and all persons designated as authors qualify for authorship, and all those who are eligible for authorship are listed.

Funding

This study was supported by AstraZeneca Pharmaceuticals, the University of Nottingham and a BBSRC CASE award. AstraZeneca Pharmaceuticals had a role in the study design.

Acknowledgments

We would like to thank Professor Sheila M. Gardiner from The University of Nottingham for her valuable help with the animal work in study 2.

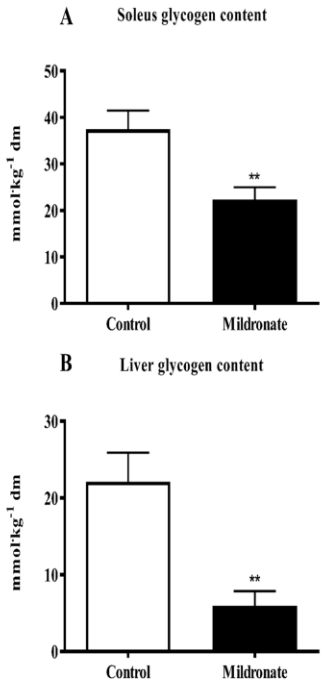

Figure 1

Figure 1. Soleus (A) and liver (B) glycogen content in control (*n*=8) and mildronate (*n*=8) treated lean Zucker rats. Values are expressed as means ± SEM. ** Significantly different from control (*P*<0.01).

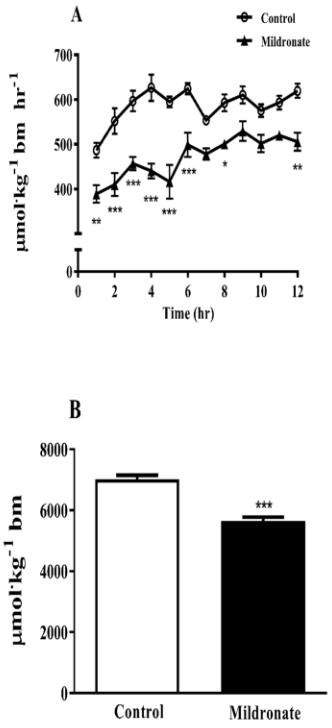

Figure 2

Figure 2. A. The rate of whole-body fat oxidation in control (*n*=8) and mildronate (*n*=8) treated lean Zucker rats over a 12 hr period. Animals were allowed to acclimatise to their metabolic cages over the course of days 7 to 10 to ensure metabolic stability, and for the final 12 hr period were fasted to circumvent confounding effects of between-group differences in food intake on metabolic rate and patterns of substrate oxidation over this 12 hr period. Values are mean ± SEM. Fat oxidation was significantly less throughout in mildronate compared to control (Main effect treatment, *P*<0.001; 2-way ANOVA). *, **, *** Significantly different from control (*P*<0.05, *P*<001; *P*<0.001, respectively).

B. B. Total fat oxidation in control (*n*=8) and mildronate (*n*=8) treated lean Zucker rats. Values are means ± SEM. *** Significantly different from control (*P*<0.001).

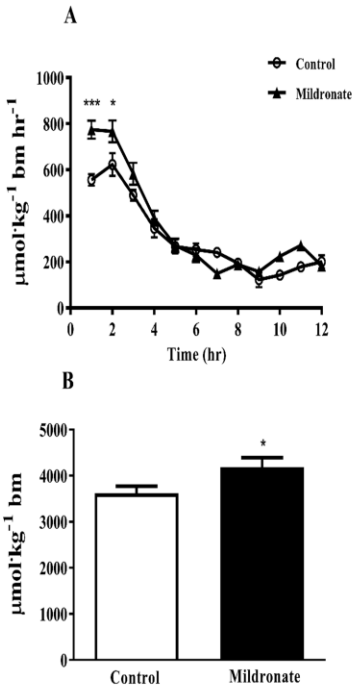

Figure 3

Figure 3. A. The rate of whole-body carbohydrate oxidation in control (*n*=8) and mildronate (*n*=8) treated lean Zucker rats over a 12 hr period. Animals were allowed to acclimatise to their metabolic cages over the course of days 7 to 10 to ensure metabolic stability, and for the final 12 hr period were fasted to circumvent confounding effects of between-group differences in food intake on metabolic rate and patterns of substrate oxidation over this 12 hr period. Values are

mean ± SEM. Carbohydrate oxidation was significantly greater in mildronate compared to control (Main effect treatment $P<0.05$; 2-way ANOVA). *, *** Significantly different from control group ($P<0.05$; $P<0.001$, respectively).

B. Total carbohydrate oxidation in control ($n=8$) and mildronate ($n=8$) treated lean Zucker rats. Values are means ± SEM. * Significantly different from control ($P<0.05$).

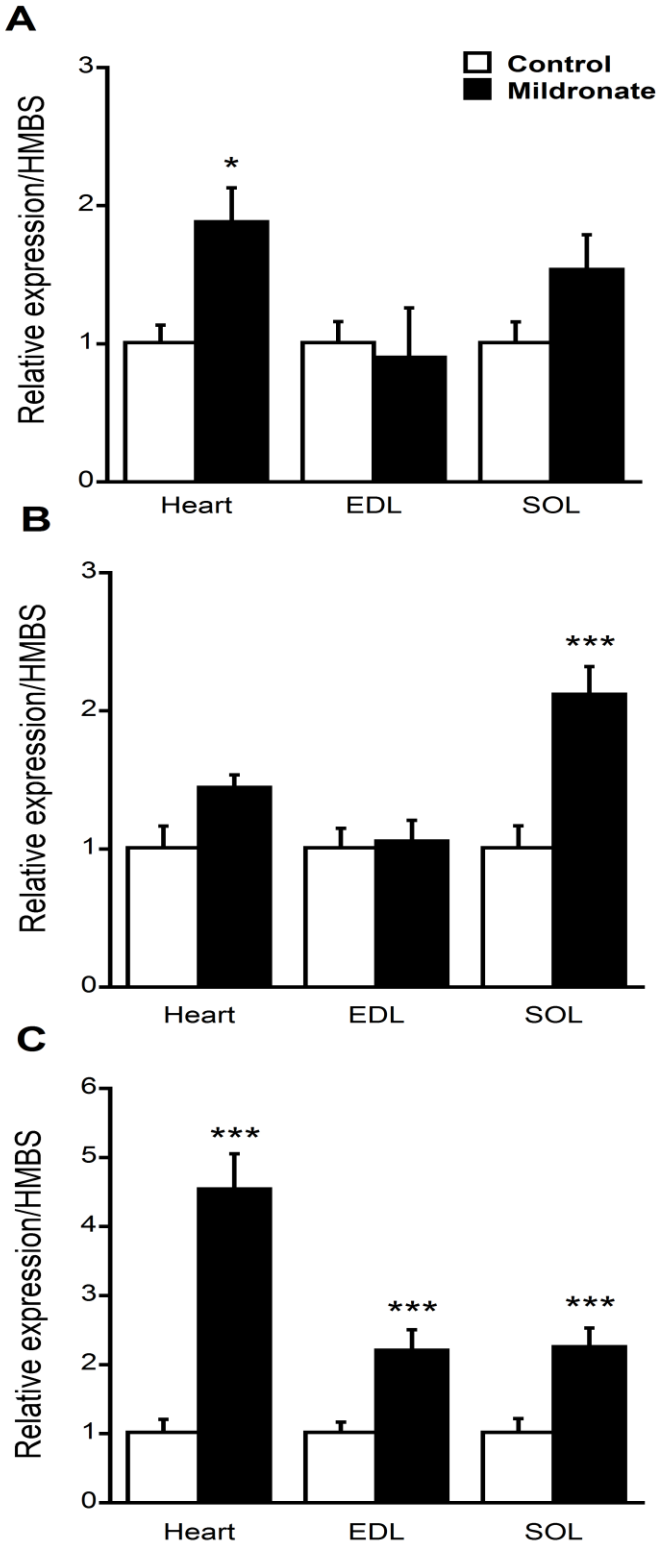

Figure 4

Figure 4. Muscle OCTN2 (A), CPT1 (B) and PDK4 (C) mRNA expression in heart, extensor digitorum longus (EDL) and soleus (soleus) in control (*n*=8) and mildronate (*n*=8) treated Wistar rats. Values are mean ± SEM. *, *** Significantly different from corresponding control value (*P*<0.05 and *P*<0.001, respectively).

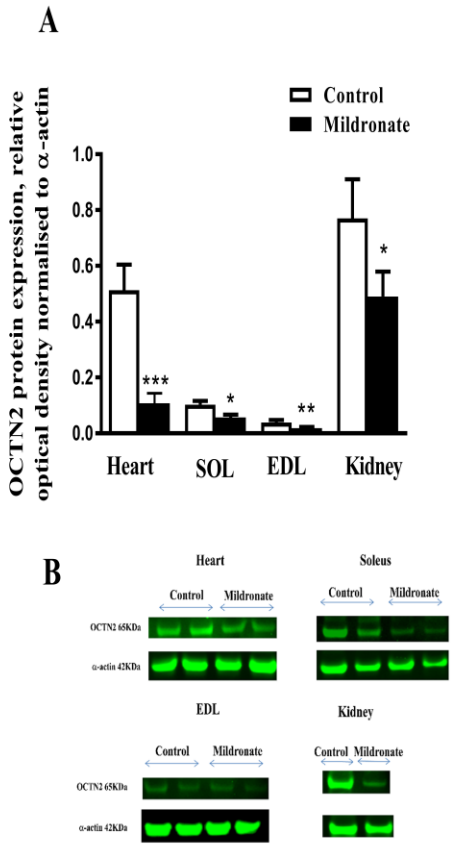

Figure 5. A. Muscle OCTN2 protein expression in heart, extensor digitorum longus (EDL), soleus and kidney in control (*n*=8) and mildronate (*n*=8) treated Wistar rats. Values are mean ± SEM. Kidney (*n*=2) is present as a positive internal control. Values are expressed as relative optical density normalised to α-actin. *, **, *** Significantly different from corresponding control value (*P*<0.05, *P*<0.01, *P*<0.001, respectively).

B. Representative blots of OCTN2 located at 63 kDa in heart, extensor digitorum longus (EDL), soleus and kidney.

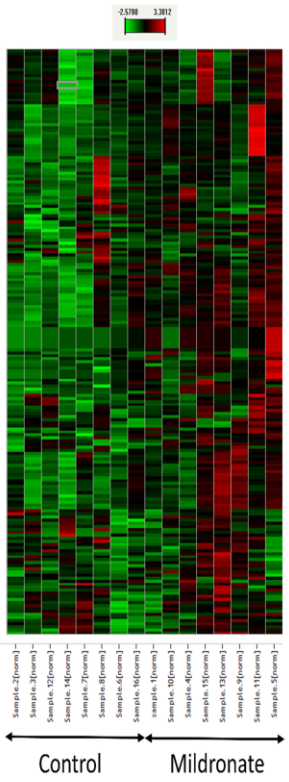

Figure 6

Figure 6. Graphical representation of data reflecting mRNA abundance in the form of colours (heat map) relative to housekeeping genes in soleus muscle of individual control animals (left on the x-axis, *n*=8) and individual mildronate treated animals (right on the x-axis, *n*=8). Red colour signifies greater relative abundance, while green signifies less relative abundance.

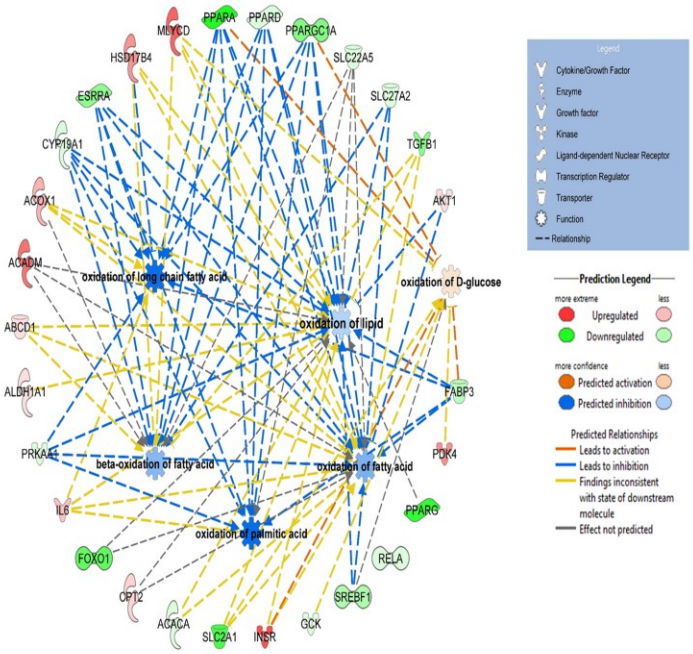

Figure 7

Figure 7. Ingenuity Pathway Analysis prediction of energy metabolism in soleus muscle based upon changes in mRNA expression from control in mildronate treated animals. The schematic highlights the most differentially regulated mRNAs (outer ring), and the predicted metabolic events resulting from these changes. Abbreviations represent as follow: PPARA, PPRD, PPARG - peroxisome proliferator-activated receptor α, δ and γ; PPARGC1A - PPARG Coactivator 1α; SLC22A5 - solute carrier family 22 Member 5 (carnitine transporter); SL27A2 - Very Long-Chain-Fatty-Acid-CoA Ligase; TGFB1 - transforming growth factor beta 1; AKT1 - Akt serine-threonine protein kinase 1; FABP3 - fatty acid binding protein 3; PDK4 - pyruvate dehydrogenase complex isoform 4; SREBF1 - sterol regulatory element binding transcription

factor 1; GCK - glucokinase, INSR - insulin receptor; SLC2A1 - solute carrier family 2 member 1; ACACA - acetyl-CoA carboxylase α; CPT2 - carnitine palmitoyl transferase 2, FOXO1 - forkhead box O1; IL6 - interleukin 6; PRKAA1 - protein kinase AMP-activated catalytic subunit α1; ALDH1A1 - aldehyde dehydrogenase 1 family member A1; ABCD1 - ATP binding cassette subfamily D member 1; ACADM - acyl-CoA dehydrogenase C4 to C12 straight chain; ACOX1 - acyl-CoA oxidase 1; CYP19A1 - cytochrome P450 family 19 subfamily A member 1.

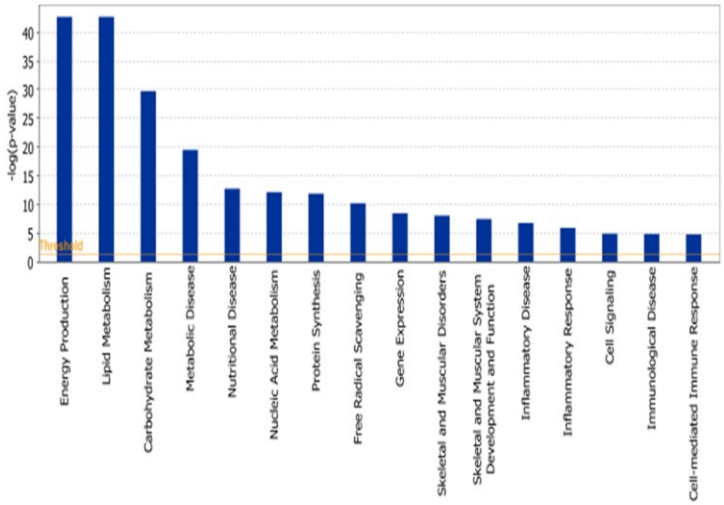

Figure 8

Figure 8. Cellular functions identified by Ingenuity Pathway Analysis as being altered from control (*n*=8) in soleus muscle of mildronate treated animals (*n*=8) based on mRNA expression data generated using the low-density microarray cards. The x-axis displays cellular functions most affected by mildronate administration, while the y-axis displays the -log of the *p*-value. The -log of p-value was calculated by Fisher's exact test right-tailed ($P<0.05$).

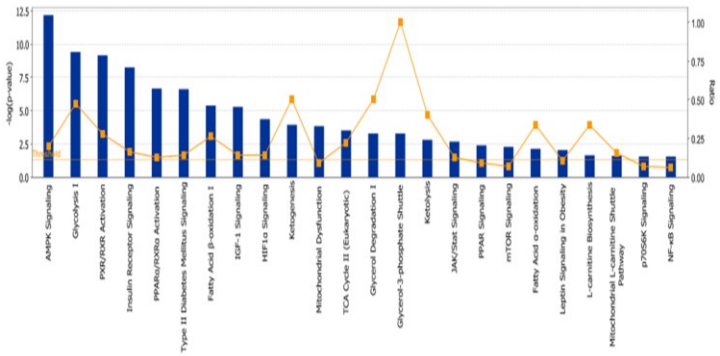

Figure 9. Metabolic pathways identified by Ingenuity Pathway Analysis as being altered from control (*n*=8) in soleus muscle of mildronate treated animals (*n*=8) based on mRNA expression data generated using the low-density microarray cards. The x-axis displays those pathways most affected by mildronate administration. The y-axes display: (1) on the left the -log of the *p*-values. The *p*-value for a given metabolic pathway was calculated by considering the number of focus transcripts that participated in the pathway and the total number of transcripts known to be associated with that pathway in Ingenuity's knowledge base. The -log of p-value was calculated using Fisher's exact test (right-tailed). The threshold was set at $P<0.05$. (2) On the right the ratio of the number of genes in a given pathway that meet cut-off criteria ($P<0.05$), divided by the total number of genes that make up that pathway.

Table 1. Carnitine ester content in the soleus muscle of control (*n*=8) and mildronate (*n*=8) treated lean Zucker rats.

	Control	Mildronate
Free carnitine	3.47±0.24	0.35±0.03***
Long-chain acylcarnitine	0.27±0.06	0.10±0.03*
Acetylcarnitine	1.11±0.20	0.54±0.06*
Total carnitine	4.86±0.13	0.99±0.05***

Values are mean ± S.E.M. Carnitine content expressed as mmol·kg^{-1} dry muscle. *, *** Significantly different from the corresponding control value (P<0.05, P<0.001 respectively).

Table 2. Muscle carnitine ester content in the heart, extensor digitorum longus (EDL) and soleus of control (*n*=8) and mildronate (*n*=8) treated Wistar rats.

	Free carnitine		Long-chain acylcarnitine		Acetylcarnitine		Total carnitine	
	Control	Mildronate	Control	Mildronate	Control	Mildronate	Control	Mildronate
Heart	4.29±0.27	0.44±0.03***	0.39±0.05	0.11±0.04***	0.84±0.11	0.49±0.10*	5.52±0.25	1.04±0.11***
EDL	3.59±0.17	0.49±0.04***	0.50±0.08	0.18±0.05**	0.46±0.09	0.19±0.03*	4.55±0.19	0.86±0.10***
Soleus	3.03±0.10	0.47±0.03***	0.29±0.05	0.20±0.04*	0.51±0.05	0.38±0.03*	3.84±0.08	1.05±0.08***

Values are mean ± S.E.M. Carnitine content expressed as mmol kg^{-1} dry muscle. *, **, *** Significantly different

from corresponding control value (P<0.05, P<0.01 and P<0.001, respectively).

Table 3. Muscle ATP, PCr and glycogen content in the heart, extensor digitorum longus (EDL), and soleus of control (*n*=8) and mildronate (*n*=8) treated Wistar rats.

	ATP		PCr		Glycogen	
	Control	Mildronate	Control	Mildronate	Control	Mildronate
Heart	16.6±0.5	18.3±1.1	6.8±0.8	11.4±1.1	93.3±7.9	66.6±4.8*
EDL	25.4±1.0	26.0±1.0	72.8±4.8	76.2±7.2	113.5±10.4	83.5±8.4*
soleus	14.4±1.1	15.3±1.3	40.2±3.1	38.3±3.7	80.1±5.9	59.5±8.1*

Values are mean ± SEM. Contents are expressed as mmol kg^{-1} dry muscle. * Significantly different from the corresponding control value (P<0.05)